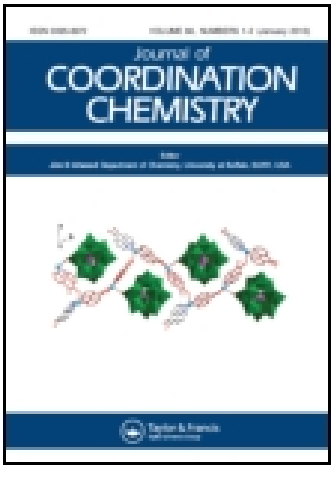

Journal of Coordination Chemistry
Publication details, including instructions for authors and subscription information:
http://www.tandfonline.com/loi/gcoo20

Synthesis, crystal structures, and biological activity of oxovanadium(V) complexes with similar tridentate hydrazone ligands

Gui-Hua Sheng[a], Xiao Han[b], Zhonglu You[c], Hai-Hua Li[c] & Hai-Liang Zhu[a]

[a] School of Life Sciences, Shandong University of Technology, ZiBo, PR China

[b] Liaoning Grain and Oil Inspection and Monitoring Department, Shenyang, PR China

[c] Department of Chemistry and Chemical Engineering, Liaoning Normal University, Dalian, PR China

Accepted author version posted online: 22 Apr 2014.Published online: 13 May 2014.

To cite this article: Gui-Hua Sheng, Xiao Han, Zhonglu You, Hai-Hua Li & Hai-Liang Zhu (2014) Synthesis, crystal structures, and biological activity of oxovanadium(V) complexes with similar tridentate hydrazone ligands, Journal of Coordination Chemistry, 67:10, 1760-1770, DOI: 10.1080/00958972.2014.916795

To link to this article: http://dx.doi.org/10.1080/00958972.2014.916795

Journal of Coordination Chemistry, 2014
Vol. 67, No. 10, 1760–1770, http://dx.doi.org/10.1080/00958972.2014.916795

Synthesis, crystal structures, and biological activity of oxovanadium(V) complexes with similar tridentate hydrazone ligands

GUI-HUA SHENG†, XIAO HAN‡, ZHONGLU YOU*§, HAI-HUA LI§ and HAI-LIANG ZHU*†

†School of Life Sciences, Shandong University of Technology, ZiBo, PR China
‡Liaoning Grain and Oil Inspection and Monitoring Department, Shenyang, PR China
§Department of Chemistry and Chemical Engineering, Liaoning Normal University, Dalian, PR China

(*Received 20 December 2013; accepted 1 April 2014*)

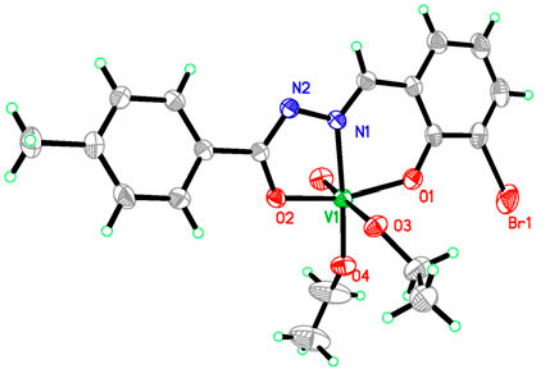

Two new oxovanadium(V) complexes, [VOL^1(OEt)(EtOH)] (**1**) and [VOL^2(OMe)(MeOH)] (**2**), were prepared by reaction of [VO(acac)$_2$] (where acac = acetylacetonate) with *N*′-(3-bromo-2-hydroxybenzylidene)-4-methylbenzohydrazide (H_2L^1) in ethanol and *N*′-(3-bromo-2-hydroxybenzylidene)-4-methoxybenzohydrazide (H_2L^2) in methanol, respectively. Crystal and molecular structures of the complexes were determined by elemental analysis, infrared spectra, and single-crystal X-ray diffraction. The V ions have octahedral coordination. Thermal stability and the inhibition of urease of the complexes were studied.

Keywords: Hydrazone ligand; Oxovanadium complex; Crystal structure; Thermal property; Urease inhibition

*Corresponding authors. Email: youzhonglu@lnnu.edu.cn (Z. You); zhuhl@nju.edu.cn (H.-L. Zhu)

1. Introduction

Urease has important negative effects on humans, stockbreeding, and agriculture [1–4]. Control of the activity of urease through the use of inhibitors could counteract these negative effects. Metal complexes have proved to be a kind of versatile enzyme inhibitor [5]. Among metal complexes, those derived from hydrazones have received particular attention in biological and medicinal chemistry [6–9]. In recent years, vanadium complexes have been reported to have interesting biological activities such as normalizing the high blood glucose levels and acting as models of haloperoxidases [10–12]. Ara and co-workers reported that some binuclear vanadium(IV) complexes possess interesting urease inhibitory activities [13]. Aslam and co-workers reported that Schiff bases of the hydrazone type also possess urease inhibitory activities [14]. Recently, our research group reported a few vanadium complexes with urease inhibitory activities [15, 16]. In order to further evaluate the structure-activity relationship on the urease inhibitory activities of vanadium complexes with hydrazone ligands, in the present article, two new oxovanadium(V) complexes, [VOL^1(OEt)(EtOH)] (**1**) and [VOL^2(OMe)(MeOH)] (**2**) (H_2L^1 = *N*′-(3-bromo-2-hydroxybenzylidene)-4-methylbenzohydrazide (H_2L^1), H_2L^2 = *N*′-(3-bromo-2-hydroxybenzylidene)-4-methoxybenzohydrazide; scheme 1), are presented.

2. Experimental

2.1. *Materials and measurements*

Commercially available 3-bromosalicylaldehyde, 4-methylbenzohydrazide, and 4-methoxybenzohydrazide were purchased from Aldrich and used without purification. Other solvents and reagents were made in China and used as received. C, H, and N elemental analyses were performed with a Perkin–Elmer elemental analyzer. Infrared spectra were recorded on a Nexus 870 FT-IR spectrometer as KBr pellets from 4000 to 400 cm^{-1}. ^{1}H NMR spectra were recorded on a Bruker instrument at 500 MHz. Thermal stability analysis was performed on a Perkin–Elmer Pyris Diamond TG–DTA thermal analysis system.

2.2. *Synthesis of H_2L^1*

3-Bromosalicylaldehyde (1.0 mM, 0.20 g) and 4-methylbenzohydrazide (1.0 mM, 0.15 g) were dissolved in methanol (30 mL) with stirring. The mixture was stirred for 30 min at

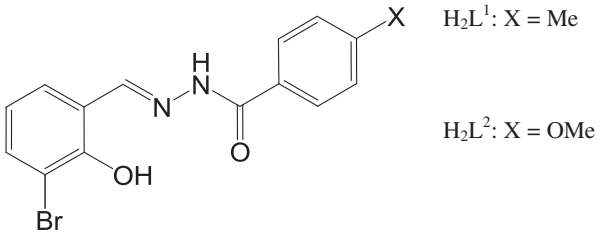

Scheme 1. The hydrazone ligands.

room temperature to give a clear solution. The solvent was evaporated to give colorless crystalline product. Yield: 95%. M.p. 228–230 °C. Analysis: Found: C 53.9%, H 4.0%, N 8.5%. Calculated for $C_{15}H_{13}BrN_2O_2$: C 54.1%, H 3.9%, N 8.4%. ^{1}H NMR data (d^6-DMSO, δ, ppm): 2.40 (s, 3H), 6.92 (t, 1H), 7.37 (d, 2H), 7.50 (d, 1H), 7.63 (d, 1H), 7.88 (d, 2H), 8.58 (s, 1H), 12.32 (s, 1H), 12.66 (s, 1H). Selected IR data (KBr, cm^{-1}): 3365 (w), 3249 (w), 1648 (s), 1610 (s), 1601 (s), 1555 (m), 1510 (s), 1448 (w), 1439 (w), 1359 (m), 1315 (m), 1293 (w), 1285 (w), 1258 (s), 1178 (s), 1138 (w), 1023 (m), 962 (w), 882 (w), 848 (m), 773 (m), 733 (m), 676 (w), 619 (w), 590 (w), 566 (w), 481 (w).

2.3. *Synthesis of H_2L^2*

3-Bromosalicylaldehyde (1.0 mM, 0.20 g) and 4-methoxybenzohydrazide (1.0 mM, 0.17 g) were dissolved in methanol (30 mL) with stirring. The mixture was stirred for 30 min at room temperature to give a clear solution. The solvent was evaporated to give colorless crystalline product. Yield: 92%. Analysis: Found: C 51.5%, H 3.7%, N 8.1%. Calculated for $C_{15}H_{13}BrN_2O_3$: C 51.6%, H 3.8%, N 8.0%. M.p. 193–194 °C. ^{1}H NMR data (d^6-DMSO, δ, ppm): 3.86 (s, 3H), 6.92 (t, 1H), 7.11 (d, 2H), 7.51 (d, 1H), 7.62 (d, 1H), 7.96 (d, 2H), 8.57 (s, 1H), 12.29 (s, 1H), 12.71 (s, 1H). Selected IR data (KBr, cm^{-1}): 3382 (*w*), 3207 (w), 1647 (s), 1613 (s), 1555 (m), 1510 (w), 1445 (m), 1386 (w), 1356 (m), 1322 (*w*), 1294 (m), 1277 (s), 1195 (w), 1136 (m), 1070 (w), 1029 (m), 956 (w), 880 (w), 768 (*w*), 732 (s), 675 (m), 619 (w), 590 (w), 525 (w), 475 (w).

2.4. *Synthesis of [VOL^1(OEt)(EtOH)]*

An ethanolic solution (10 mL) of [$VO(acac)_2$] (0.1 mM, 26.5 mg) was added to an ethanolic solution (10 mL) of H_2L^1 (0.1 mM, 33.3 mg) with stirring. The mixture was stirred for 30 min at room temperature to give a deep brown solution. The resulting solution was allowed to stand in air for a few days. Brown block-shaped crystals suitable for X-ray single-crystal diffraction were formed at the bottom of the vessel. The isolated product was washed three times with cold ethanol and dried in air. Yield: 53%. Analysis: Found: C 46.8%, H 4.7%, N 5.6%. Calculated for $C_{19}H_{22}BrN_2O_5V$: C 46.6%, H 4.5%, N 5.7%. Selected IR data (KBr, cm^{-1}): 3195 (br, w), 1603 (vs), 1588 (m), 1538 (w), 1500 (s), 1483 (w), 1429 (s), 1390 (m), 1380 (m), 1340 (s), 1283 (m), 1230 (w), 1192 (w), 1178 (w), 1140 (m), 1087 (w), 1043 (s), 1003 (w), 972 (m), 915 (m), 856 (w), 830 (w), 778 (w), 739 (m), 686 (w), 650 (w), 629 (w), 592 (m), 562 (w), 487 (w), 457 (w), 408 (w).

2.5. *Synthesis of [VOL^2(OMe)(MeOH)]*

This complex was prepared by the same method as that described for [VOL^1(OEt)(EtOH)], but with ethanol replaced by methanol and H_2L^1 replaced by H_2L^2 (0.1 mM, 34.9 mg). Yield: 65%. Analysis: Found: C 42.7%, H 3.9%, N 5.7%. Calculated for $C_{17}H_{18}BrN_2O_6V$: C 42.8%, H 3.8%, N 5.9%. Selected IR data (KBr, cm^{-1}): 3178 (br, w), 1609 (vs), 1538 (m), 1506 (s), 1489 (s), 1458 (w), 1428 (m), 1416 (w), 1333 (s), 1271 (s), 1253 (m), 1231 (w), 1171 (m), 1141 (w), 1050 (w), 1030 (2), 979 (m), 973 (m), 910 (w), 841 (m), 771 (w), 739 (m), 687 (m), 659 (w), 628 (w), 598 (s), 577 (m), 559 (w), 483 (w), 466 (w), 434 (w).

Table 1. Crystallographic data and refinement parameters for **1** and **2**.

Complex	**1**	**2**
Chemical formula	$C_{19}H_{22}BrN_2O_5V$	$C_{17}H_{18}BrN_2O_6V$
Mr	489.2	477.2
Crystal color, habit	Brown, block	Brown, block
Crystal size (mm^3)	0.20 × 0.17 × 0.15	0.10 × 0.07 × 0.06
Crystal system	Triclinic	Triclinic
Space group	*P-1*	*P-1*
Unit cell parameters		
a (Å)	8.195(2)	8.233(2)
b (Å)	10.432(2)	11.580(2)
c (Å)	12.942(3)	13.001(2)
α (°)	88.308(6)	103.954(12)
β (°)	71.752(6)	101.532(7)
γ (°)	84.633(6)	109.703(8)
V ($Å^3$)	1046.2(4)	1077.5(3)
Z	2	2
d_{Calcd} ($g\,cm^{-3}$)	1.553	1.471
Temperature (K)	298(2)	298(2)
μ (mm^{-1})	2.415	2.346
F (0 0 0)	496	480
Number of unique data	3881	3504
Number of observed data [$I > 2\sigma(I)$]	2951	2324
Number of parameters	259	248
Number of restraints	1	13
R_1, wR_2 [$I > 2\sigma(I)$]	0.0504, 0.1114	0.0881, 0.2360
R_1, wR_2 (all data)	0.0727, 0.1233	0.1253, 0.2679
Goodness of fit on F^2	1.009	1.039

2.6. *X-ray crystallography*

Diffraction intensities for the complexes were collected at 298(2) K using a Bruker D8 VENTURE PHOTON diffractometer with Mo *Kα* radiation ($\lambda = 0.71073$ Å). The collected data were reduced using SAINT [17] and multi-scan absorption corrections were performed using SADABS [18]. The structures were solved by direct methods and refined against F^2 by full-matrix least-squares using SHELXTL [19]. C16 and C17 of **2** were refined in an isotropic manner due to disorder. The remaining non-hydrogen atoms in both complexes were refined anisotropically. The methanol and ethanol hydrogens in both structures were located from difference Fourier maps and refined isotropically, with O–H distances restrained to 0.85(1) Å. The remaining hydrogens were placed in idealized positions and constrained to ride on their parent atoms. The crystallographic data for the complexes are summarized in table 1. Selected bond lengths and angles are given in table 2.

2.7. *Urease inhibitory activity assay*

Helicobacter pylori (ATCC 43504; American Type Culture Collection, Manassas, VA) was grown in brucella broth supplemented with 10% heat-inactivated horse serum for 24 h at 37 °C under microaerobic condition (5% O_2, 10% CO_2, and 85% N_2). The method of preparation of *H. pylori* urease by Mao was followed [20]. Briefly, broth cultures (50 mL, 2.0×10^8 CFU mL^{-1}) were centrifuged (5000 *g*, 4 °C) to collect the bacteria, and after washing twice with phosphate-buffered saline (pH 7.4), the *H. pylori* precipitate was stored at −80 °C. While the *H. pylori* was returned to room temperature, and mixed with 3 mL of

Table 2. Selected bond distances (Å) and angles (°) for **1** and **2**.

1			
V(1)–O(1)	1.872(3)	V(1)–O(2)	1.955(2)
V(1)–O(3)	2.315(3)	V(1)–O(4)	1.757(3)
V(1)–O(5)	1.577(3)	V(1)–N(1)	2.133(3)
C(7)–N(1)	1.282(4)	N(1)–N(2)	1.395(4)
C(8)–N(2)	1.303(4)	C(8)–O(2)	1.299(4)
O(5)–V(1)–O(4)	101.1(1)	O(5)–V(1)–O(1)	99.6(1)
O(4)–V(1)–O(1)	103.6(1)	O(5)–V(1)–O(2)	98.9(1)
O(4)–V(1)–O(2)	95.2(1)	O(1)–V(1)–O(2)	150.3(1)
O(5)–V(1)–N(1)	91.6(1)	O(4)–V(1)–N(1)	164.5(1)
O(1)–V(1)–N(1)	82.6(1)	O(2)–V(1)–N(1)	74.0(1)
O(5)–V(1)–O(3)	177.7(1)	O(4)–V(1)–O(3)	80.8(1)
O(1)–V(1)–O(3)	81.0(1)	O(2)–V(1)–O(3)	79.5(1)
N(1)–V(1)–O(3)	86.2(1)	C(7)–N(1)–N(2)	116.4(3)
N(1)–N(2)–C(8)	108.3(3)	N(2)–C(8)–O(2)	123.2(3)
2			
V(1)–O(1)	1.860(6)	V(1)–O(2)	1.940(6)
V(1)–O(4)	1.774(6)	V(1)–O(5)	1.587(6)
V(1)–O(6)	2.357(6)	V(1)–N(1)	2.129(6)
C(7)–N(1)	1.275(10)	N(1)–N(2)	1.381(8)
C(8)–N(2)	1.303(10)	C(8)–O(2)	1.313(9)
O(5)–V(1)–O(4)	102.5(3)	O(5)–V(1)–O(1)	99.9(3)
O(4)–V(1)–O(1)	102.4(3)	O(5)–V(1)–O(2)	98.5(3)
O(4)–V(1)–O(2)	94.3(3)	O(1)–V(1)–O(2)	151.7(2)
O(5)–V(1)–N(1)	94.8(3)	O(4)–V(1)–N(1)	160.4(3)
O(1)–V(1)–N(1)	83.3(2)	O(2)–V(1)–N(1)	73.8(2)
O(5)–V(1)–O(6)	174.7(3)	O(4)–V(1)–O(6)	82.4(3)
O(1)–V(1)–O(6)	80.7(2)	O(2)–V(1)–O(6)	79.2(2)
N(1)–V(1)–O(6)	80.1(2)	C(7)–N(1)–N(2)	118.2(6)
N(1)–N(2)–C(8)	109.8(6)	N(2)–C(8)–O(2)	120.8(7)

distilled water and protease inhibitors, sonication was performed for 60 s. Following centrifugation (15000 *g*, 4 °C), the supernatant was desalted through a Sephadex G–25 column (PD–10 columns, Amersham–Pharmacia Biotech, Uppsala, Sweden). The resultant crude urease solution was added to an equal volume of glycerol and stored at 4 °C until used in the experiment. The mixture, containing 25 µL (4U) of *H. pylori* urease and 25 µL of the test compound, was pre-incubated for 3 h at room temperature in a 96-well assay plate. Urease activity was determined by measuring ammonia production by the indophenol method.

2.8. *Docking simulations*

Molecular docking of **2** with the 3-D structure of *jack bean* urease (entry 3LA4 in the Protein Data Bank) was carried out using the DOCK 4.2 program suite [21, 22]. The graphical user interface AutoDockTools (ADT 1.4.5) was performed to setup every inhibitor–enzyme interaction, where all hydrogens were added. Gasteiger charges were calculated and non-polar hydrogens were merged to carbon atoms. The Ni initial parameters are set as $r = 1.170$ Å, $q = +2.0$, and *van der Waals* well depth of 0.100 kcal M^{-1}. As performed by the graphical user interface AutoDockTools, the catalytic center and the peripheral anionic site of the target protein were scanned to evaluate the modeled binding mode of the inhibitor–urease complex. The flexible docking of the ligand structure was done by the Lamarckian genetic algorithm, searching for favorable bonding conformations of the ligand at the sites of the target protein.

3. Results and discussion

3.1. *General*

Replacement of two acetylacetonates in $[VO(acac)_2]$ by hydrazones in ethanol or methanol resulted in the formation of two structurally similar complexes. The complexes are soluble in DMF, DMSO, methanol, ethanol, and acetonitrile. Molar conductances of **1** and **2** at the concentrations of 10^{-4} M are 13 and 22 $\Omega^{-1}\,cm^2\,M^{-1}$, respectively, indicating they are non-electrolytes [23].

3.2. *Crystal structure description of the complexes*

The molecular structures and atom numbering schemes of **1** and **2** are shown in figures 1 and 2, respectively. The V ions in the complexes are octahedral, with the three donors of the hydrazone ligands and one deprotonated solvent defining the equatorial plane, and with one oxo and one solvent occupying the axial positions. The distance between V(1) and O(5) is 1.58 Å, indicating typical V=O bonds. The V(1)–O(3) bonds in **1** and the V(1)–O(6) bonds in **2** are significantly longer than the other V–O bonds, yet, it is not uncommon for such complexes [24, 25]. The coordination bond lengths in the complexes are comparable to each other and also similar to those observed in mononuclear oxovanadium(V) complexes with octahedral coordination [24–30]. The angular distortion in the octahedral environment around V comes from the five- and six-membered chelate rings formed by the benzohydrazone ligands. For the same reason, the *trans* angles significantly deviate from ideal values of 180°. Distortion of the octahedral coordination can be observed from the coordinate bond angles, ranging from 74.0(1)° to 103.6(1)° for the perpendicular angles and

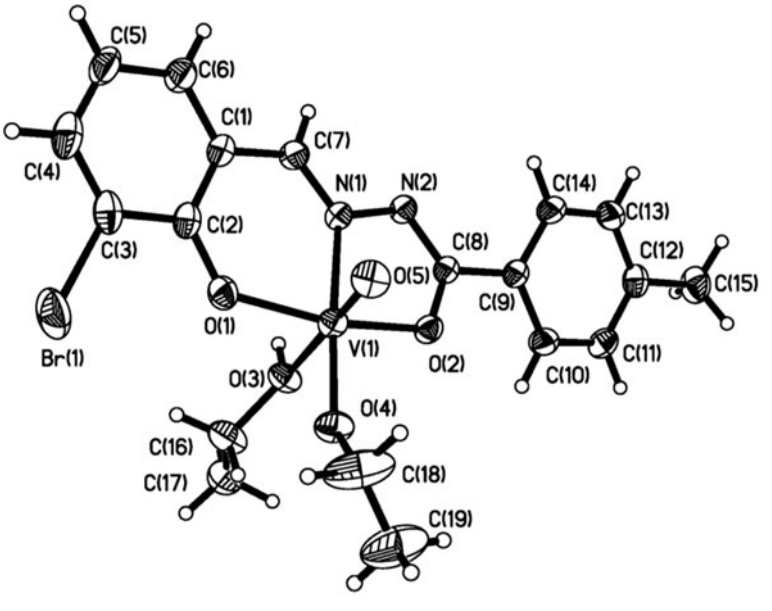

Figure 1. ORTEP plot of the crystal structure of **1**. Displacement ellipsoids of non-hydrogen atoms are drawn at the 30% probability level.

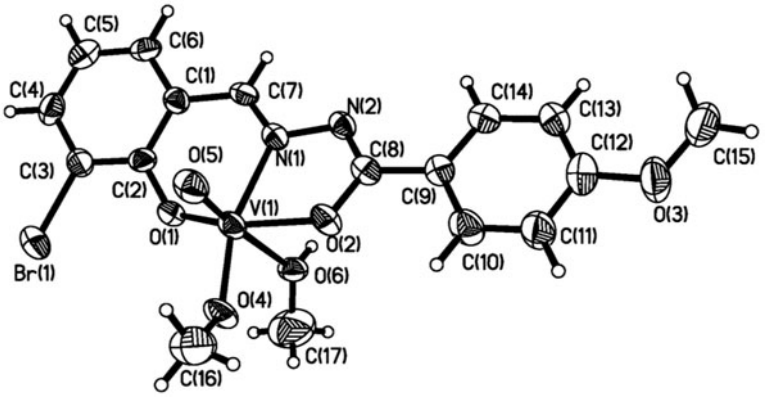

Figure 2. ORTEP plot of the crystal structure of **2**. Displacement ellipsoids of non-hydrogen atoms are drawn at the 30% probability level.

from 150.3(1)° to 177.7(1)° for the diagonal angles for **1**, and from 73.8(2)° to 102.4(3)° for the perpendicular angles and from 151.7(2)° to 174.7(3)° for the diagonal angles for **2**. The displacement of V from the equatorial plane is 0.275(1) Å for **1** and 0.307(1) Å for **2**. The formation of bonds with V, together with delocalization of the ligand, leads to planarity of the hydrazone. The dihedral angles between the substituted benzene rings are 9.1(2)° for **1** and 13.3(3)° for **2**. In the crystal structures of the complexes, adjacent molecules are linked through intermolecular O–H···N hydrogen bonds [for **1**: O(3)–H(3) = 0.85(1) Å, H(3)···N(2)^{i} = 1.98(1) Å, O(3)···N(2)^{i} = 2.816(4) Å, O(3)–H(3)···N(2)^{i} = 170(5)°; symmetry code for i: $2-x$, $-y$, $-z$; for **2**: O(6)–H(6) = 0.85(1) Å, H(6)···N(2)^{ii} = 2.02(2) Å, O(6)···N(2)^{ii} = 2.863(9) Å, O(6)–H(6)···N(2)^{ii} = 171(10)°; symmetry code for ii: $1-x$, $-y$, $1-z$], forming a dimer.

3.3. *IR spectra*

The hydrazones showed stretching bands attributed to C=O, C=N, C–OH, and NH at 1647, 1613, 1180 and 1260–1280, and 3210–3250 cm^{-1}, respectively. Both complexes exhibit typical bands at 972 cm^{-1} for **1** and 973 cm^{-1} for **2**, assigned to V=O vibration. The bands due to $\nu_{C=O}$ and ν_{NH} were absent in the complexes, but new C–O stretches appeared at 1283 cm^{-1} for **1** and 1271 cm^{-1} for **2**. This suggests *keto*-imine tautomerization of the ligands during complexation. The $\nu_{C=N}$ absorption at 1610 cm^{-1} (H_2L^1) and 1613 cm^{-1} (H_2L^2) in the free benzohydrazones shifted to 1603 cm^{-1} for **1** and 1609 cm^{-1} for **2** upon coordination. The weak peaks in the low wavenumber region 400–650 cm^{-1} may be attributed to V–O and V–N bonds in the complexes.

3.4. *Thermal property*

Differential thermal (DT) and thermal gravimetric analyses (TGA) were conducted to examine the stability of **1** and **2** (figure 3 for **1** and figure 4 for **2**). For **1**, the first step starting at 240 °C and ending at 426 °C, with 18.8% weight loss, might be caused by loss of the neutral and deprotonated ethanols (18.6%). The complex decomposed from 430 to 515 °C,

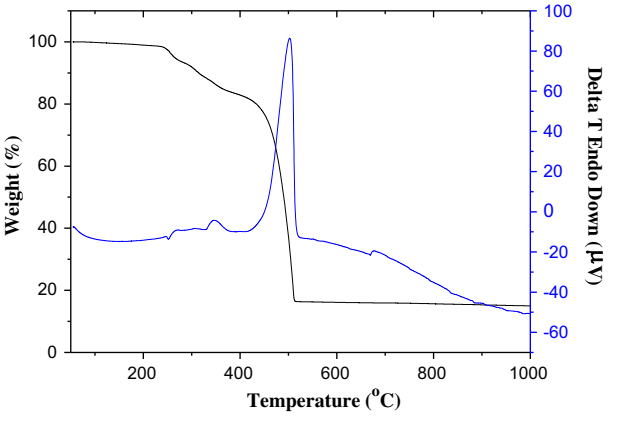

Figure 3. DT–TGA curve of **1**.

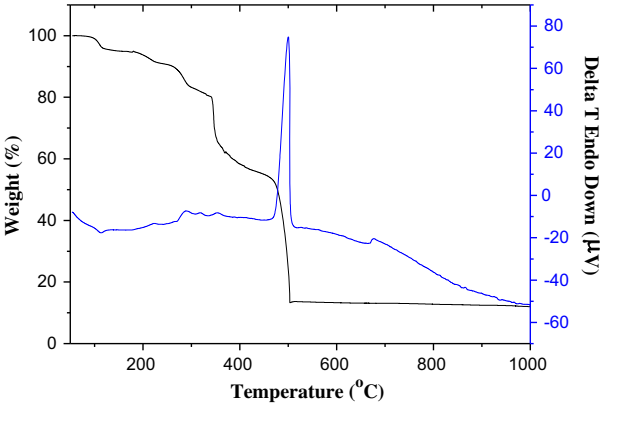

Figure 4. DT–TGA curve of **2**.

corresponding to loss of hydrazone and formation of V_2O_5. The total observed weight loss of 83.2% is close to the calculated value of 81.4%. For **2**, the complex was first decomposed from 93 to 285 °C, with a weight loss of 14.0%, which might be from loss of the neutral and deprotonated methanol ligands (13.3%). The complex decomposed from 290 to 510 °C, corresponding to loss of hydrazone and formation of V_2O_5. The total observed weight loss of 83.3% is close to the calculated value of 81.2%.

3.5. *Pharmacology*

The results of urease inhibition are summarized in table 3. Compared with the reference inhibitor acetohydroxamic acid (AHA), the free hydrazones and the vanadyl sulfate have very weak interactions against urease. Complexes **1** and **2** at concentration of 100 μM L^{-1} have urease inhibitory activities with percent inhibition of 32 ± 3 and 62 ± 3, respectively, and with an IC_{50} value of 31.0 μM L^{-1} for **2**. It is clear that the activity of **2** is stronger than that of **1** and near to that of AHA.

Table 3. Inhibition of urease by the tested materials.

Tested materials	Percent inhibition*	IC_{50} ($\mu M\ L^{-1}$)
1	32 ± 3	–
2	62 ± 3	43.0
H_2L^1	17 ± 2	–
H_2L^2	15 ± 3	–
Vanadyl sulfate	26 ± 2	220
AHA	88 ± 4	37.5

*Concentration of the tested material is 100 $\mu M\ L^{-1}$.

3.6. *Molecular docking study*

The binding model of **2** with *jack bean* urease was simulated using the Dock program, revealing that the complex is well filled in the active pocket of the urease. Additional interactions have been established in a variety of conformations because of the flexibilities of the complex and the amino acid residues of the urease. The optimized cluster (20 occurrences) was ranked by energy level in the best conformation of the inhibitor–urease model structures, where the binding energy is $-6.0\ kcal\ M^{-1}$. Some hydrophobic interactions also exist in the corresponding inhibitor–urease complex. The binding mode of the complex in the enzyme active site is shown in figures 5 and 6. The oxo forms a hydrogen bond with *ASP*223. In addition, the complex forms some hydrophobic interactions and other weak interactions with the amino acid residues. In contrast, no hydrogen bond was found between **1** and the amino acid residues of the urease active site. This probably causes the activity difference of the complexes.

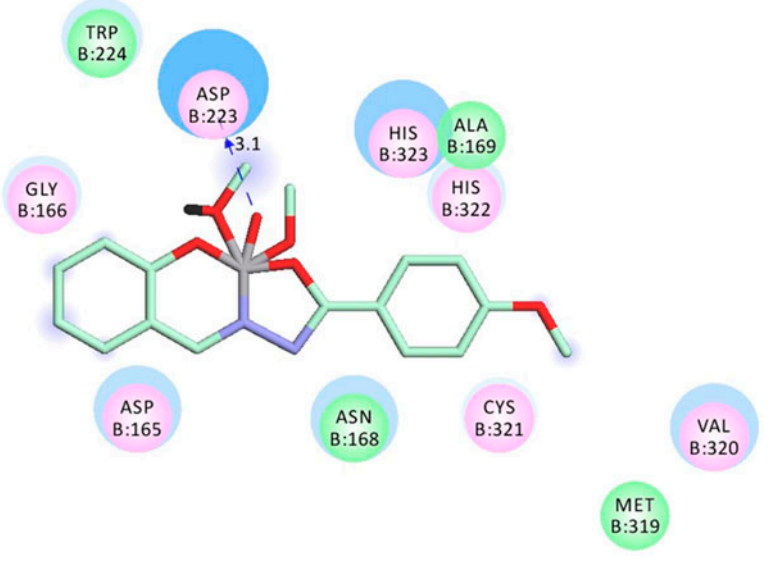

Figure 5. The interaction between **2** and the *ASP*223 residue of the urease.

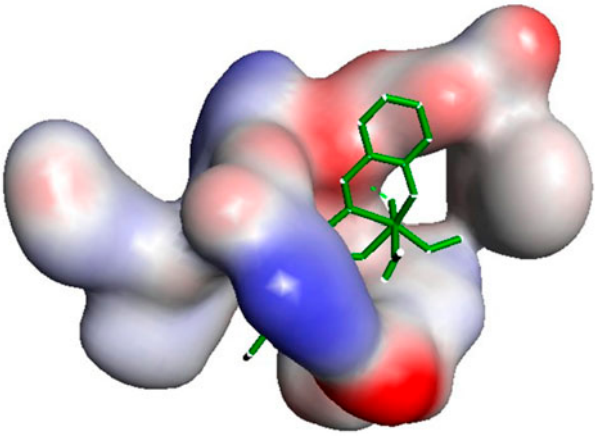

Figure 6. The interaction between **2** (stick) and the active pocket (surface) of the urease.

4. Conclusion

Two new oxovanadium(V) complexes with similar tridentate hydrazone ligands have been prepared and structurally characterized. The hydrazones coordinate to V through phenolate O, imino N, and enolate O. Complex **2** may be used as a potential urease inhibitor with an IC_{50} value of 43.0 μM L^{-1}.

Supplementary material

CCDC–978059 (**1**) and 978060 (**2**) contain the supplementary crystallographic data for this article. These data can be obtained free of charge at http://www.ccdc.cam.ac.uk/const/retrieving.html or from the Cambridge Crystallographic Data Centre (CCDC), 12 Union Road, Cambridge CB2 1EZ, UK; Fax: +44(0)1223336033 or E-mail: deposit@ccdc.cam.ac.uk.

Supplemental data

Supplemental data for this article can be accessed http://dx.doi.org/10.1080/00958972.2014.916795.

References

[1] S.S. Francisco, O. Urrutia, V. Martin, A. Peristeropoulos, J.M. Garcia-Mina. *J. Sci. Food Agric.*, **91**, 1569 (2011).
[2] Z.-P. Xiao, T.-W. Ma, W.-C. Fu, X.-C. Peng, A.-H. Zhang, H.-L. Zhu. *Eur. J. Med. Chem.*, **45**, 5064 (2010).
[3] T.G. Barros, J.S. Williamson, O.A.C. Antunes, E.M.F. Muri. *Lett. Drug Des. Discovery*, **6**, 186 (2009).

[4] J.C. Polacco, P. Mazzafera, T. Tezotto. *Plant Sci.*, **199–200**, 79 (2013).
[5] A.Y. Louie, T.J. Meade. *Chem. Rev.*, **99**, 2711 (1999).
[6] M.F. Wang, Z.Y. Yang, Y. Li, H.G. Li. *J. Coord. Chem.*, **64**, 2974 (2011).
[7] A. El-Dissouky, O. Al-Fulaij, M.K. Awad, S. Rizk. *J. Coord. Chem.*, **63**, 330 (2010).
[8] K.M. Ibrahim, I.M. Gabr, R.R. Zaky. *J. Coord. Chem.*, **62**, 1100 (2009).
[9] A.S. El-Tabl, F.A. El-Saied, A.N. Al-Hakimi. *J. Coord. Chem.*, **61**, 2380 (2008).
[10] P. Caravan, L. Gelmini, N. Glover, F.G. Herring, H.L. Li, J.H. McNeill, S.J. Rettig, I.A. Setyawati, E. Shuter, Y. Sun, A.S. Tracey, V.G. Yuen, C. Orvig. *J. Am. Chem. Soc.*, **117**, 12759 (1995).
[11] A.A. Nejo, G.A. Kolawole, A.R. Opoku, C. Muller, J. Wolowska. *J. Coord. Chem.*, **62**, 3411 (2009).
[12] A. Messerschmidt, L. Prade, R. Wever. *Biol. Chem.*, **378**, 309 (1997).
[13] R. Ara, U. Ashiq, M. Mahroof-Tahir, Z.T. Maqsood, K.M. Khan, M.A. Lodhi, M.I. Choudhary. *Chem. Biodivers.*, **4**, 58 (2007).
[14] M.A.S. Aslam, S. Mahmood, M. Shahid, A. Saeed, J. Iqbal. *Eur. J. Med. Chem.*, **46**, 5473 (2011).
[15] Z.-L. You, D.-H. Shi, J.-C. Zhang, Y.-P. Ma, C. Wang, K. Li. *Inorg. Chim. Acta*, **384**, 54 (2012).
[16] Z.-L. You, H. Sun, B.-W. Ding, Y.-P. Ma, M. Zhang, D.-M. Xian. *J. Coord. Chem.*, **64**, 3510 (2011).
[17] Bruker. *SMART and SAINT*, Bruker AXS Inc., Madison, WI (2002).
[18] G.M. Sheldrick. *SADABS. Program for Empirical Absorption Correction of Area Detector*, University of Göttingen, Germany (1996).
[19] G.M. Sheldrick. *Acta Crystallogr., Sect. A: Found. Crystallogr.*, **64**, 112 (2008).
[20] W.-J. Mao, P.-C. Lv, L. Shi, H.-Q. Li, H.-L. Zhu. *Bioorg. Med. Chem.*, **17**, 7531 (2009).
[21] R. Huey, G.M. Morris, A.J. Olson, D.S. Goodsell. *J. Comput. Chem.*, **28**, 1145 (2007).
[22] G. Estiu, D. Suárez, K.M. Merz. *J. Comput. Chem.*, **27**, 1240 (2006).
[23] W.J. Geary. *Coord. Chem. Rev.*, **7**, 81 (1971).
[24] Y. Zhao, X. Han, X.-X. Zhou, H.-H. Li, Z.-L. You. *Chin. J. Inorg. Chem.*, **29**, 867 (2013).
[25] H.H. Monfared, S. Alavi, R. Bikas, M. Vahedpour, P. Mayer. *Polyhedron*, **29**, 3355 (2010).
[26] A. Sarkar, S. Pal. *Polyhedron*, **25**, 1689 (2006).
[27] Y.-M. Cui, Y.-J. Cai, W. Chen. *J. Coord. Chem.*, **64**, 1385 (2011).
[28] M.R. Maurya, S. Agarwal, C. Bader, M. Ebel, D. Rehder. *Dalton Trans.*, 537 (2005).
[29] H. Guo, J. Lu, Z. Ruan, Y. Zhang, Y. Liu, L. Zang, J. Jiang, J. Huang. *J. Coord. Chem.*, **65**, 191 (2012).
[30] Y. Deng, Y. Yang, Y. Zhang, Q. Yan, J. Liu. *J. Coord. Chem.*, **65**, 1409 (2012).